Potential Antiviral Lignans from the Roots of Saururus chinensis with Activity against Epstein-Barr Virus Lytic Replication

ARTICLE *in* JOURNAL OF NATURAL PRODUCTS · DECEMBER 2013

Impact Factor: 3.8 · DOI: 10.1021/np400757k · Source: PubMed

6 AUTHORS, INCLUDING:

Taizong Wu
Sun Yat-Sen University
5 PUBLICATIONS **9** CITATIONS
SEE PROFILE

Jun Xu
Sun Yat-Sen University
102 PUBLICATIONS **808** CITATIONS
SEE PROFILE

Yan Yuan
University of Pennsylvania
44 PUBLICATIONS **1,880** CITATIONS
SEE PROFILE

Qiong Gu
Sun Yat-Sen University
57 PUBLICATIONS **384** CITATIONS
SEE PROFILE

JOURNAL OF NATURAL PRODUCTS

Article

pubs.acs.org/jnp

Potential Antiviral Lignans from the Roots of *Saururus chinensis* with Activity against Epstein−Barr Virus Lytic Replication

Hui Cui,[†] Bo Xu,[‡] Taizong Wu,[†] Jun Xu,[†] Yan Yuan,*[,‡,§] and Qiong Gu*[,†]

[†]Research Center for Drug Discovery, School of Pharmaceutical Sciences, Sun Yat-sen University, Guangzhou 510006, People's Republic of China

[‡]The Institute of Human Virology, Zhongshan School of Medicine, Sun Yat-sen University, Guangzhou, Guangdong 510080, People's Republic of China

[§]Department of Microbiology, School of Dental Medicine, University of Pennsylvania, Philadelphia, Pennsylvania 19104, United States

Supporting Information

ABSTRACT: Epstein−Barr virus (EBV) is a member of the γ-herpes virus subfamily and has been implicated in the pathogenesis of several human malignancies. Bioassay-guided fractionation was conducted on an EtOAc-soluble extract of the roots of *Saururus chinensis* and monitored using an EBV lytic replication assay. This led to the isolation of 19 new (**1**−**19**) and nine known (**20**−**28**) lignans. The absolute configurations of the new lignans were established by Mosher's ester, ECD, and computational methods. Eight lignans, including three sesquineolignans (**19**, **23**, and **24**) and five dineolignans (**3**, **4**, **26**, **27**, and **28**), exhibited inhibitory effects toward EBV lytic replication with EC_{50} values from 1.09 to 7.55 μM and SI values from 3.3 to 116.4. In particular, manassantin B (**27**) exhibited the most promising inhibition, with an EC_{50} of 1.72 μM, low cytotoxicity, CC_{50} > 200 μM, and SI > 116.4. This is the first study demonstrating that lignans possess anti-EBV lytic replication activity.

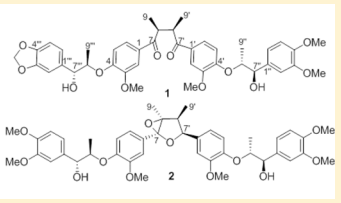

Saururus chinensis Baill (Saururaceae) is a perennial herbaceous plant distributed in China and Korea. It has been used in traditional Chinese medicine as an antipyretic, diuretic, and anti-inflammatory agent to treat diseases such as edema, jaundice, and gonorrhea.[1] Previous photochemical investigations on species of this genus led to the isolation of different types of compounds, including lignans, aristolactams, flavonoids, anthraquinones, and furanoditerpenes.[1] Lignans are the main active constituents of *S. chinensis*. Some have exhibited a broad spectrum of biological activities including NF-κB,[1] HIV-1 protease,[2] arginase II,[3] and HIF-1 inhibitory activities,[4] cardiovascular effects,[5] and cytotoxic activity.[6]

Epstein−Barr virus (EBV) is a γ-herpes virus associated with several human diseases, including infectious mononucleosis, Burkitt lymphoma, T-cell lymphoma, Hodgkin's disease, nasopharyngeal carcinoma, and gastric carcinoma.[7] EBV has two modes of infection, latent and lytic viral replication.[8] When EBV enters the lytic cycle, the viral genome is amplified and virus particles are produced.[9] Therefore, reactivation of the lytic cycle of EBV may play a role in the pathogenesis of malignancies.[10−12] Two nucleotide analogues, acylovir and ganciclovir, are used to treat herpesvirus infections in clinical practice.[13,14] Some natural products, including 4-*O*-acetyl-7-acetoxychavicol,[15] triterpenoids,[16] sesquiterpenoids,[17] and isoflavonoids,[18] have been demonstrated to inhibit EBV lytic replication.

As part of continuing studies to identify antivirals from medicinal plants,[19,20] the 95% EtOH extract from the roots of *S. chinensis* demonstrated potent inhibition of EBV replication with an EC_{50} value of 34.38 μg/mL in P3HR-1 cell lines. Bioactivity-guided fractionation of the EtOH extract using an EBV lytic replication assay led to the isolation of 19 new (**1**−**19**) and nine known lignans (**20**−**28**). Eight lignans, including sesquineolignans **19**, **23**, and **24** and dineolignans **3**, **4**, **26**, **27**, and **28**, demonstrated significant inhibitory effects toward EBV lytic replication. Herein, the isolation and structure elucidation of the new compounds (**1**−**19**) and the anti-EBV lytic replication activities of all the isolates are reported.

RESULTS AND DISCUSSION

The 95% EtOH extract was separated into four portions according to polarity by dissolving it in petroleum ether, EtOAc, *n*-BuOH, and H_2O, and each fraction was assayed for antiviral activity. The EtOAc-soluble fraction exhibited the most potent anti-EBV activity with an EC_{50} of 21.31 μg/mL. Bioactivity-guided fractionation of the EtOAc extract using the EBV lytic DNA replication assay led to the isolation of 19 new (**1**−**19**) and nine known lignans (**20**−**28**).

The known compounds were identified as schinlignin A (**20**),[21] epigrandisin (**21**),[22] di-*O*-methyltetrahydrofuriguaiacin B (**22**),[23] saucerneol methyl ether (**23**),[24] saucerneol D (**24**),[24] (7*S*,8*S*)-polysphorin (**25**),[1] manassantin A (**26**),[25] manassantin B (**27**),[25] and 4-*O*-demethylmanassantin B (**28**)[4] by spectroscopic analysis and comparison with literature data.

Received: September 16, 2013
Published: December 20, 2013

Table 1. ^{1}H and ^{13}C NMR Chemical Shifts of Compounds 1−4 and 19[a]

	1		2		3		4		19	
position	δ_H (J in Hz)	δ_C	δ_H (J in Hz)	δ_C	δ_H (J in Hz)	δ_C	δ_H (J in Hz)	δ_C	δ_H (J in Hz)	δ_C
1		130.7		132.0		136.6		136.8		136.4
2	7.54, d (1.9)	111.7	6.92, m	111.1	6.93, m	118.9	6.92, m	110.3	6.92, d (1.7)	111.2
3		150.6		149.2		150.8		150.8		150.6
4		152.0		146.9		146.8		146.5		145.6
5	7.01, m	116.0	7.02, d (8.1)	118.7	6.78, m	111.1	6.97, d (8.1)	118.8	6.92, m	118.6
6	7.67, d (6.3)	123.0	6.92, m	120.1	6.93, m	118.9	6.99, d (8.1)	118.8	6.86, m	119.7
7		203.1		106.8	5.46, d (5.8)	83.5	5.46, d (5.8)	83.5	5.12, d (8.6)	83.0
8	3.91, m	43.6		82.3	2.30, m	44.4	2.30, m	44.3	1.79, m	46.1
9	1.31, d (6.0)	16.1	0.75, s	19.6	0.72, d (6.1)	15.0	0.72, d (6.1)	15.0	0.65, d (6.9)	15.1
1′		130.7		134.8		136.6		136.6		132.1
2′	7.54, d (1.9)	111.7	6.92, m	111.1	6.94, m	110.4	6.92, m	110.3	7.01, d (1.7)	109.6
3′		150.6		149.2		149.1		150.8		146.7
4′		152.1		147.9		146.8		146.3		146.7
5′	7.01, m	116.1	6.92, m	110.7	6.85, m	110.4	6.84, m	119.1	6.86, m	114.3
6′	7.67, d (6.3)	123.0	6.92, m	119.4	6.92, m	118.9	6.99, d (8.1)	118.8	6.97, m	119.4
7′		203.0	5.33, d (7.8)	79.9	5.46, d (5.8)	83.5	5.46, d (5.9)	83.5	4.39, d (9.3)	87.5
8′	3.91, m	43.5	2.87, m	46.2	2.30, m	44.4	2.30, m	44.3	2.25, m	47.8
9′	1.31, d (6.0)	16.1	0.65, d (5.6)	11.4	0.72, d (6.1)	15.0	0.72, d (6.1)	15.0	1.05, d (6.5)	15.1
1″		133.7		132.6		132.2		133.6		132.1
2″		110.1	6.84, m	110.3	6.86, m	109.7	6.92, m	113.7	6.92, m	109.6
3″		149.2		150.7		146.7		145.7		146.7
4″		149.3		149.1		145.7		146.6		145.4
5″	6.85, m	111.1	6.84, d (8.0)	111.1	6.80, m	114.5	6.78, m	108.2	6.93, m	114.4
6″	6.94, m	120.0	6.91, m	120.1	6.87, m	120.1	6.87, m	119.1	6.99, m	120.8
7″	4.70, d (9.0)	78.2	4.65, d (7.1)	78.5	4.63, d (8.3)	78.6	4.61, d (8.2)	77.4	4.60, d (8.3)	78.5
8″	4.32, m	82.6	4.15, m	83.8	4.13, m	84.2	4.13, m	84.1	4.10, m	84.0
9″	1.20, d (6.9)	16.7	1.21, d (6.1)	17.2	1.17, d (6.1)	17.2	1.16, d (6.1)	17.0	1.13, d (6.2)	17.1
1‴		132.3		132.5		132.8		134.1		
2‴	6.92, brs	107.6	6.84, m	110.3	6.83, m	110.4	6.78, m	107.7		
3‴		148.0		150.7		149.2		147.9		
4‴		147.7		149.1		150.8		147.5		
5‴	6.79, d (7.9)	108.3	6.84, d (8.0)	111.1	6.83, m	110.4	6.76, m	110.6		
6‴	6.85, m	121.1	6.91, m	120.1	6.80, m	120.8	6.78, m	121.2		
7‴	4.68, d (9.3)	78.2	4.65, d (7.1)	78.5	4.63, d (8.3)	78.6	4.62, d (8.2)	78.6		
8‴	4.32, m	82.8	4.22, m	84.0	4.13, m	84.4	4.13, m	84.2		
9‴	1.20, d (6.9)	16.8	1.18, d (6.2)	17.1	1.17, d (6.1)	17.2	1.16, d (6.1)	17.1		
OMe-3/3′	3.89, s	56.1	3.89, s	56.1	3.92, s	56.1	3.92, s	56.0	3.84, s	56.1
OMe-3″/4″	3.89, s	56.1	3.89, s	56.1	3.89, s	56.1	3.89, s	56.1	3.88, s	56.0
OMe-3‴/4‴			3.87, s	56.1	3.87, s	56.1				
CH_2O−	5.96, s	101.2					5.94, s	101.2		
−OH					5.63, brs		5.61, brs		5.72, brs	

[a] ^{1}H NMR measured at 400 MHz, ^{13}C NMR measured at 100 MHz, obtained in $CDCl_3$ with TMS as internal standard. Assignments were supported with HSQC and HMBC NMR spectra.

Compound **1** was obtained as a white powder. Its HRESIMS showed a sodiated molecular ion at m/z 753.3044, corresponding to the molecular formula $C_{41}H_{46}O_{12}Na$. Its IR spectrum exhibited absorptions for hydroxy (3449 and 3367 cm^{-1}) and conjugated carbonyl (1658 cm^{-1}) groups, as well as an aromatic ring (1511 cm^{-1}). The NMR spectra of **1** (Table 1) closely resembled those of manassantin B (**27**).[25] Comparison of the ^{13}C NMR spectra of **1** and manassantin B (**27**) revealed two carbonyls (δ_C 203.1, 203.0) in compound **1** instead of two oxymethines. These data indicated a seco-tetrahydrofuran moiety with the two carbonyl groups located at C-7 and C-7′. The HMBC correlations of H-9/9′ (δ_H 1.31, d, J = 6.0 Hz) and H-8/8′ (δ_H 3.91, m) with C-7/7′ (δ_C 203.1, 203.0), H-2 and H-6 with C-7, and H-2′ and H-6′ with C-7′ supported the above functional group assignments (Supporting Information, Figure S7). Thus, the molecular structure of **1** was elucidated as shown.

The coupling constants for H-7″ ($J_{7'',8''}$ = 9.0 Hz) and H-7‴ ($J_{7''',8'''}$ = 9.3 Hz) revealed *threo* configurations for C-7″/8″ and C-7‴/8‴.[25] The absolute configurations of C-7″ and C-7‴ were determined using the Mosher's ester method.[26] Treatment of compound **1** with (*R*)- or (*S*)-MTPA chloride in anhydrous pyridine yielded the (*S*)- and (*R*)-MTPA ester derivatives, respectively. The ^{1}H NMR chemical shift differences ($\Delta\delta_{S-R}$) between the **1***R* and **1***S* esters are shown in Figure 1. The negative $\Delta\delta$ for H-8″, H-9″, H-8‴, and H-9‴ and the positive values for 3″-OMe, 4″-OMe, and the methylenedioxy indicated the *R* configurations for both C-7″ and C-7‴. Therefore, C-8″ and C-8‴ were assigned *R* configurations.

dx.doi.org/10.1021/np400757k | J. Nat. Prod. 2014, 77, 100−110

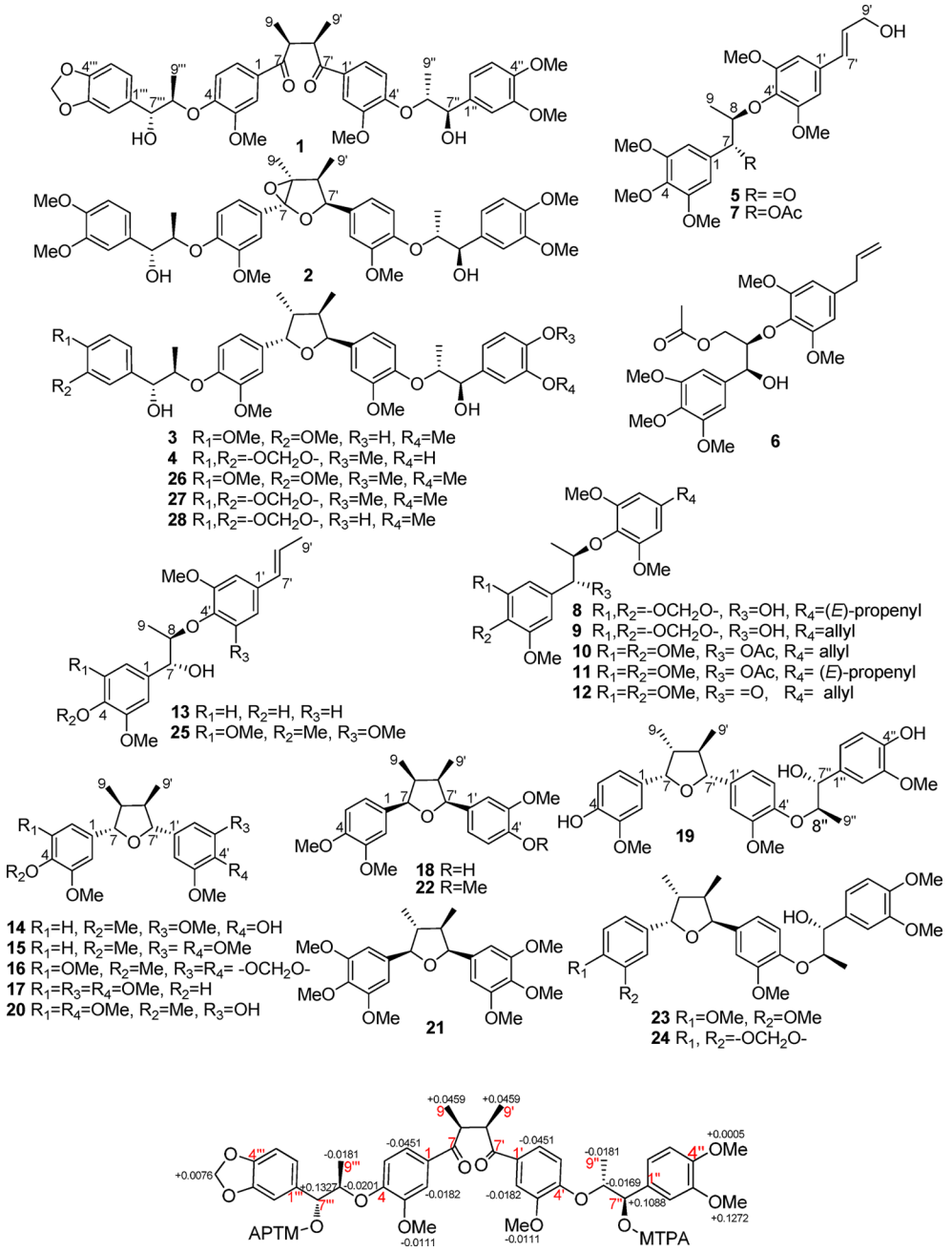

Figure 1. $\Delta\delta_{S-R}$ values of MTPA esters of **1**.

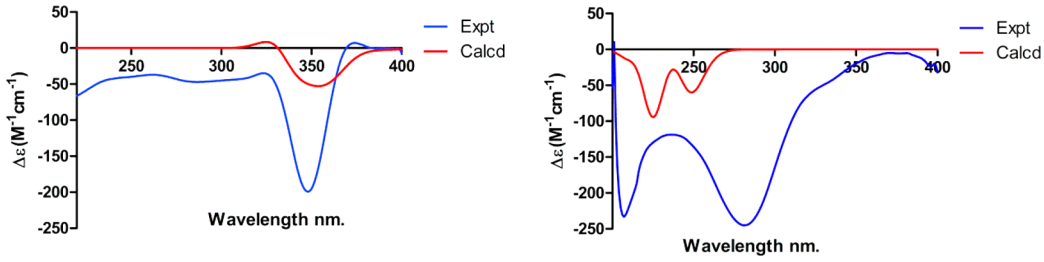

Figure 2. Experimental and calculated ECD spectra of **1** (left) and **2** (right) in MeOH.

Electronic circular dichroism (ECD) methods were used to determine the configuration of C-8/8′ in compound **1**. ECD spectra were calculated using the Gaussian 09 program at the TD-DFT-B3LYP/6-31(d,p) level in MeOH. This calculation for 8*S*,8′*R* configurations agreed with the experimental ECD data (Figure 2; Supporting Information, Figure S145). Thus, the

dx.doi.org/10.1021/np400757k | *J. Nat. Prod.* 2014, 77, 100−110

structure of compound **1** was unambiguously defined as (8*S*,8′*R*)-7,7′-dioxo-seco-manassantin B and was given the trivial name saurucinol A.

Compound **2** was obtained as a white, amorphous solid. Its molecular formula was determined to be $C_{42}H_{51}O_{12}$ from an ion at *m*/*z* 747.3362 in the HRESIMS. The NMR data of **2** (Table 1) were typical for a tetrahydrofuran-type dineolignan[23] and showed two oxygenated quaternary carbons at δ_C 106.8 and 82.3. These data indicated that the tetrahydrofuran ring is oxygenated at C-7 and C-8. Comparison of the NMR data of **2** and manassantin A (**26**)[25] revealed that compound **2** was a 7,8-epoxy derivative of **26**. HMBC correlations of CH_3-9 with the two oxygenated carbons C-7 and C-8 and C-8′ and of CH_3-9′ with C-8′, C-7′, and C-8 confirmed that the oxirane ring is located at C-7 and C-8 (Supporting Information, Figure S15).

Because of the limited quantities of compound **2**, we failed to establish the absolute configurations of C-7″/8″ and C-7‴/8‴ using the Mosher's method. The relative configurations of C-7″/7‴ and C-8″/8‴ in **2** were assumed to be *R* by comparison of their spectroscopic data (Table 1) with those of manassantin A.[25]

The relative configuration of the tetrahydrofuran ring in compound **2** was determined via a NOESY experiment. NOESY cross-peaks of H-7′/H-8′ and CH_3-9 and of H-2/H-6 and CH_3-9 indicated that the tetrahydrofuran ring assumed a *syn*−*anti*−*syn* conformation in compound **2**, similar to manassantin A analogues (Supporting Information, Figure S16).[25] The ECD data of compound **2** were also used to determine the absolute configuration of the tetrahydrofuran ring. The calculated ECD spectrum of the (7*S*,8*S*,7′*S*,8′*S*)-stereoisomer moderately agreed with the experimental ECD spectrum (Figure 2; Supporting Information, Figure S146). Thus, the structure of compound **2** was tentatively defined as *rel*-(7*S*,8*S*,7′*S*,8′*S*)-7,8-epoxymanassantin A and was assigned the trivial name saurucinol B.

Compound **3** had a molecular formula of $C_{41}H_{50}O_{11}$, as established by HRESIMS. The NMR data (Table 1) resembled those of manassantin A (**26**), except for the absence of one methoxy group in compound **3**. The ^{1}H NMR spectrum showed the presence of a phenolic hydroxy group (δ_H 5.63). In the ^{13}C NMR spectrum of manassantin A (**26**), C-3″ and C-4″ resonated at δ_C 149.1 and 148.9, respectively. However, these carbons in **3** resonated at δ_C 146.7 and 145.7, respectively. Furthermore, the chemical shift of C-5″ (δ_C 111.0) in manassantin A was shifted downfield to δ_C 114.5 in compound **3**. These characteristic ^{13}C NMR chemical shifts indicated a neolignan with 3-OMe and 4-OH substitutions.[23] The HMBC spectrum (Supporting Information, Figure S23) displayed correlations of the phenolic proton (δ_H 5.63) with the carbons corresponding to resonances at δ_C 145.7 and 114.5. These correlations implied that the phenolic hydroxy group is located at C-4″ rather than C-3″. Compound **3** and manassantin A have similar NMR spectra and negative optical rotations, suggesting that they have the same absolute configurations. The configuration of manassantin A was determined to be 7″*R*,7‴*R*,8″*R*,8‴*R*,7*S*,7′*S*,8*R*,8′*R* through synthetic methods.[27] Thus, the structure of compound **3** (4″-*O*-demethylmanassantin A) was defined as (7″*R*,7‴*R*,8″*R*,8‴*R*)-(7*S*,7′*S*,8*R*,8′*R*)-4″,7″,7‴-trihydroxy-3,3′,3″,3‴,4‴-pentamethoxy-7,7′-epoxy-4,8‴:4′,8″-dioxy-8,8′-dineolignan.

The NMR data of **4** (Table 1) were similar to those of 4-*O*-demethylmanassantin B (**28**).[4] Analysis of the NMR data of **4** and **28** revealed the presence of one hydroxy (δ_H 5.61) group in both **4** and **28**. HMBC correlations from H-7″ to C-1″ (δ_C 133.6), C-2″ (δ_C 113.7), and C-6″ (δ_C 119.1) indicated the hydroxy substitution at C-3 in **4** (Supporting Information, Figure S31). Compound **4** and 4-*O*-demethylmanassantin B had similar NMR and ECD data (Supporting Information, Figure S140) and negative optical rotations, suggesting that they have the same absolute configurations.[4] Thus, the structure of compound **4** was delineated as 3″-*O*-demethylmanassantin B.

Compound **5**, a white powder, had the molecular formula $C_{23}H_{28}O_8$, as established by HRESIMS. The NMR data were similar to those of (2,6-dimethoxy-4-propenylphenoxy)-1-(3,4,5-trimethoxyphenyl)propan-1-one (**12**) (Tables 2 and 3) except for the absence of one allyl group and the presence of an *E*-propenyl moiety.[28] The HMBC correlations of H-7′ (δ_H 6.52, d, 15.8) and H-8′ (δ_H 6.26, dt, 15.8, 5.6) with C-1′ (δ_C 132.9), H-7′ with C-2′/6′ (δ_C 103.7), and H-2′/6′ (δ_H 6.57, s) with C-7′ (δ_C 131.0) indicated that the *E*-propenyl group is located at C-1′ (Supporting Information, Figure S39). Therefore, **5** was identified as (+)-(8*R*)-3,4,5,3′,5′-pentamethoxy-$\Delta^{7',8'}$-9′-hydroxy-7-oxo-8-*O*-4′-neolignan, based on the specific rotation of +44 and ECD data, which showed a positive Cotton effect at 358 nm. Compound **5** was given the trivial name saurucinol C.

Compound **6** had the molecular formula $C_{25}H_{32}O_9$. The NMR data of **6** (Table 2) closely resembled those of *erythro*-2-(4″-allyl-2″,6″-dimethoxyphenoxy)-(3′,4′,5′-trimethoxyphenyl)propan-1,3-diol[29] except for the presence of an *O*-acetyl group. The *O*-acetyl group was connected to C-9 based on the HMBC (Supporting Information, Figure S46) correlations of a methyl (δ_H 2.05) with a hydroxymethyl (C-9, δ_C 64.1) and an acetoxy carbonyl carbon (δ_C 170.7). The coupling constant of H-7 ($J_{7,8}$ = 8.0 Hz) suggested that **6** possesses a 7,8-*threo*-configuration.[23] Moreover, in the ECD spectrum, the negative Cotton effects at 209 and 280 nm indicated the 8*R* configuration for compound **6**[30,31] (Supporting Information, Figure S141). Thus, the structure of **6** was defined as (7*R*,8*R*)-8-*O*-4′-7-(3,4,5-trimethoxyphenyl)-8-(1′-allyl-3′,5′-dimethoxy)-9-*O*-acetylpropanetriol and was assigned the trivial name saurucinol D.

Compound **7**, a white powder, had a molecular formula of $C_{25}H_{32}O_9$ by HRESIMS. The NMR data (Table 2) were similar to those of **5**, except for the absence of a carbonyl (δ_C 197.4) resonance and additional resonances for an oxymethine (δ_C 79.9; δ_H 5.85, d, 7.1) and an acetoxy group (δ_C 170.0, 21.2; δ_H 1.90, s). HMBC (Supporting Information, Figure S53) correlation from H-7 (δ_H 5.85) to the acetoxy carbonyl carbon (δ_C 170.0) indicated that the acetoxy group was located at C-7. The absolute configuration of compound **7** was determined to be 7*R*,8*R* based on the ECD data showing negative Cotton effects at 209 and 294 nm (Supporting Information, Figure S141).[30,31] Thus, based on its specific rotation of −34, the structure of compound **7** was defined as (−)-(7*R*,8*R*)-3,4,5,3′,5′-pentamethoxy-$\Delta^{7',8'}$-9′-hydroxy-7-acetoxy- 8-*O*-4′-neolignan and given the trivial name saurucinol E.

The NMR data of compound **8** (Table 2) was typical of an 8-*O*-4′-neolignan. One *E*-propenyl unit was also indicated by the NMR data. The HMBC correlations of H-2′/6′ with C-7′ and H-7′/H-8′ with C-1′ indicated that the *E*-propenyl moiety was located at C-1′ (Supporting Information, Figure S60). Furthermore, the HMBC correlations of the methylenedioxy hydrogens (δ_H 5.94, s) with C-4/C-5 indicated the C-4/C-5 location of the methylenedioxy group. The coupling constant of H-7 ($J_{7,8}$ = 8.4 Hz) indicated a 7,8-*threo* configuration. On the basis of the ECD (Supporting Information, Figure S141) and NMR data,[30,31] the structure of compound **8** was delineated as (−)-(7*R*,8*R*,7′*E*)-4,5-methylenedioxy-3,3′,5′-trimethoxy-7-hydroxy-1′-propenyl-8-*O*-4′-neolignan and was given the trivial name saurucinol F.

dx.doi.org/10.1021/np400757k | *J. Nat. Prod.* 2014, 77, 100−110

Table 2. ^{1}H and ^{13}C NMR Data (δ) for Compounds 5–9[a]

	5		6		7		8		9	
position	δ_H (J in Hz)	δ_C	δ_H (J in Hz)	δ_C	δ_H (J in Hz)	δ_C	δ_H (J in Hz)	δ_C	δ_H (J in Hz)	δ_C
1		130.5		135.5		133.8		135.6		134.9
2	7.48, d (4.6)	107.3	6.58, s	104.2	6.60, d (4.6)	104.8	6.55, s	101.7	6.55, s	101.7
3		152.9		153.3		153.2		143.4		143.6
4		142.7		137.9		138.1		134.9		136.1
5		152.9		153.3		153.3		148.9		148.8
6	7.48, d (4.6)	107.3	6.58, s	104.2	6.60, d (4.6)	104.8	6.55, s	107.0	6.55, s	107.2
7		197.4	4.98, d (8.0)	74.6	5.85, d (7.1)	79.9	4.57, d (8.4)	79.3	4.57, d (8.2)	79.3
8	5.30, q (6.7)	80.8	4.02, dd (8.0, 3.4)	86.6	4.46, m	80.3	3.91, m	86.6	3.92, m	86.5
9	1.55, d (6.6)	18.0	4.54, dd (12.0, 3.4)	64.1	1.13, d (6.6)	17.3	1.19, d (6.3)	17.7	1.19, d (6.2)	17.7
			3.94 (12.0, 2.6)							
1′		132.9		135.0		132.1		134.1		135.3
2′	6.57, s	103.7	6.42, s	105.5	6.61, d (4.7)	104.0	6.58, s	103.0	6.44, s	105.6
3′		153.3		152.6		153.3		152.9		152.8
4′		135.5		136.7		137.4		136.1		135.6
5′		153.3		152.6		153.3		152.9		152.8
6′	6.57, s	103.7	6.42, s	105.5	6.61, d (4.7)	104.0	6.58, s	103.0	6.44, s	105.6
7′	6.52, d (15.8)	131.0	3.34, d (6.6)	40.6	6.54, d (15.8)	131.3	6.34, d (15.7)	130.9	3.35, d (6.6)	40.6
8′	6.26, dt (15.8, 5.6)	128.4	5.95, m	137.0	6.28, m	128.0	6.17, qd (15.4, 6.6)	125.7	5.96, m	137.2
9′	4.30, brs	63.6	5.12, m	116.4	4.32, d (4.3)	63.8	1.89, d (6.5)	18.5	5.11, m	116.3
3/5-OMe	3.87, s	56.3	3.85, s	56.2	3.84	56.2	3.89, s	56.7	3.86, s	56.7
3′/5′-OMe	3.74, s	56.0	3.82, s	56.1	3.84	56.3	3.89, s	56.1	3.86, s	56.1
4-OMe	3.90, s	61.0	3.81, s	60.9	3.82	60.9				
CH_2O–							5.94, s	101.5	5.96, s	101.5
OAc				170.7		170.0				
OAc			2.05, s	20.9	1.90, s	21.2				

[a] ^{1}H NMR measured at 400 MHz, ^{13}C NMR measured at 100 MHz, obtained in $CDCl_3$ with TMS as internal standard. Assignments were supported with HSQC and HMBC NMR spectra.

Table 3. ^{1}H and ^{13}C NMR Data (δ) for Compounds 10–13[a]

	10		11		12		13	
position	δ_H (J in Hz)	δ_C	δ_H (J in Hz)	δ_C	δ_H (J in Hz)	δ_C	δ_H (J in Hz)	δ_C
1		133.9		133.9		130.7		132.1
2	6.61, s	104.6	6.60, s	104.7	7.50, s	107.3	6.85–6.95	109.4
3		153.2		153.2		153.0		146.9
4		137.8		137.9		142.4		145.9
5		153.2		153.2		153.0	6.85–6.95	114.2
6	6.61, s	104.6	6.60, s	104.7	7.50, s	107.3	6.85–6.95	120.9
7	5.85, d (8.8)	79.9	5.85, d (7.2)	79.9		197.9	4.61, d (8.4)	78.6
8	4.42, m	80.2	4.45, m	80.3	5.25, m	80.9	4.08, m	84.4
9	1.12, d (6.6)	17.4	1.13, d (6.4)	17.4	1.54, d (6.7)	18.0	1.16, d (6.2)	17.2
1′		135.4		133.5		133.8		133.6
2′	6.57, s	105.7	6.56, s	103.2	6.38, s	105.6	6.85–6.95	109.5
3′		153.1		153.2		153.3		151.2
4′		135.6		136.6		136.2		146.9
5′		153.1		153.2		153.3	6.85–6.95	118.9
6′	6.57, s	105.7	6.56, s	103.2	6.38, s	105.6	6.85–6.95	119.2
7′	3.33, d (6.6)	40.6	6.33, d (15.7)	131.1	3.31, d (6.2)	40.7	6.35, d (15.6)	130.6
8′	6.26, m	137.4	6.15, m	125.2	5.94, m	137.3	6.14, dt (15.6, 6.5)	125.0
9′	5.09, m	116.1	1.88, d (6.5)	18.5	5.09, m	116.2	1.87, d (6.5)	18.5
3/5-OMe	3.84, s	56.3	3.85, s	56.3	3.87, s	56.0	3. 91, s	56.0
3′/5′-OMe	3.80, s	56.2	3.82, s	56.2	3.72, s	56.4	3.90, s	56.0
4-OMe	3.82, s	60.9	3.82, s	60.9	3.90, s	61.1		
OAc		170.1		170.1				
OAc	1.92, s	21.2	1.92 (s)	21.2				

[a] ^{1}H NMR measured at 400 MHz, ^{13}C NMR measured at 100 MHz, obtained in $CDCl_3$ with TMS as internal standard. Assignments were supported with HSQC and HMBC NMR spectra.

dx.doi.org/10.1021/np400757k | J. Nat. Prod. 2014, 77, 100–110

Table 4. ^{1}H and ^{13}C NMR Data (δ) for Compounds 14−18[a]

	14		15		16		17		18	
position	δ_H (J in Hz)	δ_C	δ_H (J in Hz)	δ_C	δ_H (J in Hz)	δ_C	δ_H (J in Hz)	δ_C	δ_H (J in Hz)	δ_C
1		134.9		134.8		136.8		133.3		133.5
2	6.99, s	110.1	6.97, s	110.2	6.65, s	103.3	6.64, s	103.3	6.80, s	109.0
3		149.1		149.3		153.3		147.1		148.8
4		148.7		148.6		137.4		134.3		146.3
5	6.86, d (7.9)	111.2	6.85, d (7.9)	111.3		153.3		147.1	6.78, d (8.1)	110.9
6	6.96, d (8.2)	118.8	6.96, d (7.9)	118.9	6.65, s	103.3	6.64, s	103.3	6.84, s	118.5
7	4.52, d (6.4)	87.7	4.53, m	87.7	4.48, d (6.4)	87.5	4.48, t (5.4)	87.4	5.42, m	83.6
8	2.32, m	44.6	2.33, m	44.8	2.31, m	44.5	2.30, m	44.3	2.26, m	44.2
9	1.05, t (6.1)	13.2	1.07, d (6.4)	13.5	1.05, d (6.5)	13.2	1.02, d (6.4)	13.0	0.69, d (5.8)	14.9
1′		133.6		138.4		134.6		138.1		134.1
2′	6.66, s	103.3	6.66, s	103.6	6.62, s	106.4	6.64, s	103.4		109.8
3′		147.1		153.4		143.4		153.3		148.1
4′		134.3		138.4		138.0		137.4		144.8
5′		147.1		153.4		149.0		153.3	6.89, d (8.0)	114.1
6′	6.66, s	103.3	6.66, s	103.6	6.62, s	100.5	6.64, s	103.4	6.84, s	119.3
7′	4.50, d (6.2)	87.3	4.52, m	87.4	4.46, d (6.6)	87.4	4.48, t (5.4)	87.5	5.42, m	83.7
8′	2.32, m	44.2	2.33, m	44.2	2.30, m	44.4	2.30, m	44.4	2.26, m	44.2
9′	1.05, d (6.1)	13.1	1.03, d (6.4)	13.0	1.02, d (6.5)	12.9	1.05, d (6.4)	13.3	0.69, d (5.8)	14.9
3-OMe	3.88, s	56.1	3.88, s	56.2	3.86, s	56.2	3. 84, s	56.1	3.89, s	56.0
4-OMe	3.87, s	56.0	3.87, s	56.0	3.88, s	60.9			3.89, s	56.0
5-OMe					3.86, s	56.2	3. 84, s	56.1		
3′-OMe	3.88, s	56.4	3.85, s	56.3			3.81, s	56.3	3.88, s	56.1
4′-OMe			3.84, s	61.0			3.80, s	60.9		
5′-OMe	3.88, s	56.4	3.85, s	56.3	3.83, s	56.7	3.81, s	56.3		
CH_2O−					5.95, s	101.5				

[a] ^{1}H NMR measured at 400 MHz, ^{13}C NMR measured at 100 MHz, obtained in $CDCl_3$ with TMS as internal standard. Assignments were supported with HSQC and HMBC NMR spectra.

Compound **9** had a molecular formula of $C_{22}H_{26}O_7$, the same as that of compound **8**. Comparison of the spectroscopic data of compounds **9** and **8** (Table 2 and Experimental Section) indicated the presence of an allyl group in **9** instead of an *E*-propenyl. The structure of **9** was confirmed by 2D NMR (COSY, HMQC, and HMBC). The coupling constant of H-7 ($J_{7,8}$ = 8.2 Hz) indicated a 7,8-*threo* configuration. Its ECD spectrum did not exhibit clear Cotton effects (Supporting Information, Figure S142); thus, the Mosher's method (Supporting Information, Figure S148) was utilized to determine its absolute configuration. Thus, compound **9** was identified as (−)-(7*R*,8*R*)-4,5-methylenedioxy-3,3′,5′-trimethoxy-7-hydroxy-1′-allyl-8-*O*-4′-neolignan and was assigned the trivial name saurucinol G.

Compound **10** had the molecular formula $C_{25}H_{32}O_8$. Its NMR data (Table 3) were similar to those of (7*R*,8*R*)-raphidecursinol B[28] except for the presence of an acetoxy group (δ_H 1.92; δ_C 170.1, 21.2). The acetoxy group was located at C-7 based on the HMBC correlations of H-7 (δ_H 5.85) and a CH_3 (δ_H 1.92) with the carbonyl carbon at δ_C 170.1. Thus, compound **10** was identified as (−)-(7*R*,8*R*)-7-*O*-acetylraphidecursinol B based on comparison of its specific rotation of −18 and spectroscopic data with those of (7*R*,8*R*)-raphidecursinol B.[28] This is the first time that compound **10** has been isolated from nature; thus it is a new natural product.

Compound **11** had the molecular formula $C_{25}H_{32}O_8$. The NMR data (Table 3) revealed the presence of an *E*-propenyl group in **11**. Compound **11** was synthesized to determine the absolute configuration of polysphorin.[28] Thus, on the basis of the specific rotation of −24, the structure of compound **11** was defined as (−)-(7*R*,8*R*)-7-*O*-acetylpolysphorin. Although compound **11** was reported as a semisynthetic derivative of polysphorin, it was identified as a natural product for the first time.

The NMR data of compound **12** (Table 3) were essentially identical to those of (2,6-dimethoxy-4-propenylphenoxy)-1-(3,4,5-trimethoxyphenyl)propan-1-one, which was synthesized to determine the configuration of polysphorin.[28] The 2D NMR spectra confirmed that the molecular structure of **12** is as shown. On the basis of its ECD spectrum (Supporting Information, Figure S142) and its specific rotation of +48 (*c* 0.03, $CHCl_3$),[28] compound **12** was identified as (+)-(8*R*)-(2,6-dimethoxy-4-propenylphenoxy)-1-(3,4,5-trimethoxyphenyl)propan-1-one. Compound **12** has been reported as a synthetic compound; however, this is the first report of its natural occurrence.

The NMR data of compound **13** (Table 3) were similar to machilin D.[23] The HMBC spectrum revealed that **13** had the same molecular structure as machilin D (Supporting Information, Figure S95).[23] However, the configuration of machilin D has not yet been determined. Mosher's method was employed to determine the configuration of **13**. The negative $\Delta\delta$ ^{1}H NMR values for H-8, H-9, 3′-OMe, H-7′, and H-8′ and the positive values for 3-OMe (Supporting Information, Figure S148) indicated a 7*R* configuration. The coupling constant of $J_{7,8}$ (8.4 Hz) indicated a 7,8-*threo* configuration. Thus, on the basis of the above mentioned data and a specific rotation of −88 (*c* 0.02, $CHCl_3$), compound **13** was defined as (−)-(7*R*,8*R*)-machilin D.

Compounds **14**−**18** are tetrahydrofuran-type lignans according to their NMR data (Table 4). Tetrahydrofuran-type lignans are the main components in plants of the *Saururus* genus.[23] The absolute configuration of the tetrahydrofuran ring in these compounds was determined from the ECD spectra. In addition, the configuration of the tetrahydrofuran ring was also identified

dx.doi.org/10.1021/np400757k | J. Nat. Prod. 2014, 77, 100−110

by comparing the chemical shifts of C-7/7′, C-8/8′, and C-9/9′ with reported data. The chemical shifts for the different configurations of the tetrahydrofuran-type lignans are summarized in Figure 3.[23,29,32−37]

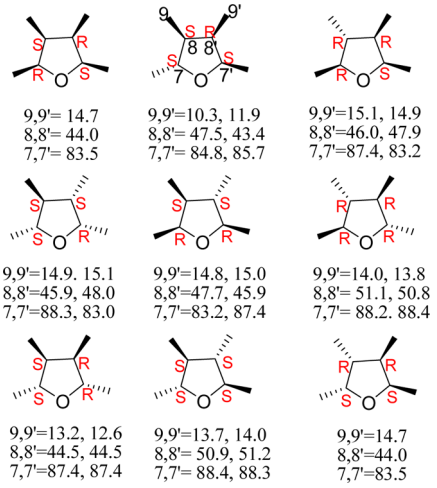

Figure 3. ^{13}C NMR chemical shifts for different configurations of the tetrahydrofuran ring.

The spectroscopic data of **14** (Table 4 and Experimental Section) were similar to those of (−)-(7*S*,7′*R*,8*S*,8′*R*)-4,4′-dihydroxy-3,3′,5′-trimethoxy-7,7′-epoxylignan[37] except for the presence of an additional methoxy group. This methoxy group was located at C-4 based on the 2D NMR data (HMQC, HMBC, and NOESY). The relative configuration of **14** was determined to be 7,8-*trans*-8,8′-*cis*-7′,8′-*trans* based on the chemical shifts, as shown in Figure 3. The NOESY spectrum of **14** (Supporting Information, Figure S103) confirmed its relative configuration. The absolute configuration of **14** was established as 7*S*,8*S*,-7′*R*,8′*R* based on comparison of its ECD data with that of (−)-(7*S*,7′*R*,8*S*,8′*R*)-4,4′-dihydroxy-3,3′,5′-trimethoxy-7,7′-epoxylignan[37] as well as with the calculated ECD spectrum (Supporting Information, Figure S147). Thus, the structure of compound **14** was defined as (−)-(7*S*,8*S*,7′*R*,8′*R*)-4′-dihydroxy-3,4,3′,5′-tetramethoxy-7,7′-epoxylignan and given the trivial name saurucinol H.

Compound **15** had the molecular formula $C_{23}H_{30}O_6$ by HRESIMS. The NMR data of compounds **15** and **14** (Table 4) were similar except for an additional methoxy group (δ_H 3.84). The methoxy group was located at C-4′ in compound **15** based on comparison of their NMR data (Table 4). The relative configuration of **15** was determined to be identical to **14** as shown. The absolute configuration of **15** was also established as 7*S*,8*S*,7′*R*,8′*R* by comparison of its ECD spectrum with that of **14** (Supporting Information, Figure S143). Accordingly, compound **15** was identified as 4-*O*-methylsaurucinol H.

The NMR data (Table 4) of compound **16** showed the presence of a methylenedioxy group. The 2D NMR (Supporting Information, Figures S115−S117) confirmed its molecular structure to be as shown. The ECD spectrum of **16** (negative Cotton effect at 227 nm) was the same as that of **14** (Supporting Information, Figure S143). Therefore, the structure of compound **16** was defined as (−)-(7*S*,8*S*,7′*R*,8′*R*)-3′,4′-methylenedioxy-3,4,5,5′-tetramethoxy-7,7′-epoxylignan and was assigned the trivial name saurucinol I.

Compound **17** had the molecular formula $C_{23}H_{30}O_7$ based on the HRESIMS data. Comparison of the NMR data of compounds **17** and **16** (Table 4) indicated that **17** was a symmetric tetrahydrofuran lignan with five methoxy groups. The IR and ^{1}H NMR data indicated the presence of a hydroxy group. The molecular structure of **17** was confirmed to be 4-hydroxy-3,5,3′,4′,5′-pentamethoxy-7,7′-epoxylignan by the 2D NMR data (HMQC, HMBC, and NOESY). The ECD spectrum of **17** showed negative Cotton effects at 223 and 277 nm, which was similar to compound **14**. Thus, the absolute configuration of **17** was defined as (−)-(7*S*,8*S*,7′*R*,8′*R*)-4-hydroxy-3,5,3′,4′,5′-pentamethoxy-7,7′-epoxylignan (Supporting Information, Figures S143, S144) and was assigned the trivial name saurucinol J.

Compound **18** had the molecular formula $C_{21}H_{26}O_5$. Through comparison of the NMR data of compounds **14**−**18**, the tetrahydrofuran ring of compound **18** had a different configuration based on the ^{13}C NMR chemical shifts of 9/9′-CH_3 (δ_C 14.9). The NMR data indicated the all-*cis* configuration of the tetrahydrofuran ring. On the basis of the ^{1}H NMR, COSY, HMBC, NOESY, and ECD spectra,[23] the structure of compound **18** was established as (7*R*,8*S*,7′*S*,8′*R*)-1-*O*-methyltetrahydrofuriguaiacin B and was given the trivial name saurucinol K.

Compound **19** was obtained as a white powder. Its spectroscopic data (UV, IR, and NMR) were essentially identical to those of saucerneol J, which was isolated from the roots of *S. chinensis*.[23] The HMBC (Supporting Information, Figure S138) and NOESY (Supporting Information, Figure S139) spectra confirmed that its molecular structure was identical to that of saucerneol J. The relative configuration of the tetrahydrofuran moiety in saucerneol J was identified as 7,8-*cis*-8,8′-*trans*-7′,8′-*trans*. Mosher's method was used to determine the absolute configurations of C-7″ and C-8″. The negative $\Delta\delta$ ^{1}H NMR values for H-8″, H-9″, H-7′, H-8′, H-9′, and 3′-OMe and the positive value for 3″-OMe indicated the 7″*R* absolute configuration (Supporting Information, Figure S148). Because of the C-7″/8″ *threo* configuration ($J_{7'',8''}$ = 8.6 Hz), C-8″ was assigned the *R* configuration. However, the absolute configurations of C-7, C-8, C-7′, and C-8′ could not be determined. Thus, compound **19** was defined as (−)-(7″*R*,8″*R*)-saucerneol J, based on its specific rotation of −86 (*c* 0.02, $CHCl_3$) and its ECD spectrum (Supporting Information, Figure S144).

The isolates were tested for their abilities to inhibit EBV lytic DNA replication in P3HR-1 cells. As shown in Table 5, all compounds showed significant to marginal inhibitory activity against EBV DNA replication, with EC_{50} values from 1.09 to 80.1 μM. Using the structural and biological data of the 28 lignans isolated in this study, the structure−activity relationships were assessed. Three sesquineolignans (**19**, **23**, and **24**) displayed significant inhibition of EBV replication with EC_{50} values of 6.95, 1.70, and 1.09 μM, respectively. Five of the seven dineolignans (**3**, **4**, **26**, **27**, and **28**) showed relatively high antiviral activities, with EC_{50} values from 1.72 to 7.55 μM. The 8-*O*-4′ neolignans (**5**−**13** and **25**) and the tetrahydrofuran-type lignans (**14**−**18** and **20**−**22**) showed moderate to weak activities, with EC_{50} values from 11.6 to 80.1 μM. These data indicated that the dineolignan or sesquineolignan scaffold is required for significant inhibition. Comparison of the structures of these five significant dineolignans (**3**, **4**, **26**, **27**, and **28**) with those of the less potent dineolignans (**1** and **2**) revealed the importance of the tetrahydrofuran ring for antiviral activity. The seco-tetrahydrofuran moiety of compound **1** and the oxirane positioned on the tetrahydrofuran ring of compound **2** led to a sharp decrease in activities (**1**, 16.2 μM; **2**, 14.5 μM), indicating that the modification of the tetrahydrofuran ring is not tolerated. The configuration of the tetrahydrofuran ring seems to be unimportant for activity, given that compounds **19**, **23**, and **24** have tetrahydrofuran rings with different

dx.doi.org/10.1021/np400757k | *J. Nat. Prod.* 2014, 77, 100−110

Table 5. Anti-EBV Lytic Replication Activities of Compounds Isolated from *S. chinensis*

no.	EC_{50}[a]	R^2[d]	CC_{50}[b]	R^2[d]	SI[c]	no.	EC_{50}[a]	R^2[d]	CC_{50}[b]	R^2[d]	SI[c]
1	16.2	0.6309	>200		12.4	**15**	67.9	0.6741	172.2	0.6141	2.5
2	14.5	0.9132	64.8	0.8692	4.4	**16**	27.3	0.7378	55.0	0.9765	2.0
3	7.55	0.9637	69.5	0.9756	9.2	**17**	29.5	0.8462	65.8	0.9195	2.2
4	2.69	0.9491	26.5	0.9038	20.2	**18**	26.9	0.9347	62.3	0.8294	2.3
5	80.1	0.9136	>200		2.5	**19**	6.95	0.9574	23.2	0.9613	3.3
6	53.3	0.7378	194.5	0.6301	3.7	**20**	16.7	0.7967	32.0	0.9725	1.9
7	44.3	0.9545	>200		4.2	**21**	25.0	0.9669	>200		8.0
8	21.7	0.8543	90.3	0.7986	4.2	**22**	49.9	0.7598	59.8	0.9140	1.2
9	12.8	0.9340	50.6	0.9027	4.0	**23**	1.70	0.9377	110.2	0.7076	65.0
10	21.5	0.9636	85.0	0.8292	4.0	**24**	1.09	0.8748	45.0	0.9263	41.1
11	25.4	0.9551	76.8	0.8448	3.0	**25**	24.0	0.9713	77.3	0.8532	3.2
12	21.9	0.8343	>200		9.1	**26**	3.42	0.9619	>200		58.5
13	23.8	0.9424	61.3	0.7890	2.6	**27**	1.72	0.9852	>200		116.4
14	11.6	0.9624	100.5	0.8751	8.6	**28**	3.52	0.9703	70.8	0.6523	20.2

[a]The inhibitory effects of the compounds against EBV lytic replication were tested and expressed as EC_{50} values (μM). [b]Cytotoxicities were measured after 2 days of compound treatments and expressed as CC_{50} values (μM). [c]Selective Index (SI) = CC_{50}/EC_{50}. [d]The regression coefficients of the dose−response curves.

configurations and all showed good activities. Furthermore, in the dineolignan series, compounds **3**, **4**, and **28**, which have a free phenolic hydroxy group, exhibited rather good inhibitory activities with EC_{50} values of 7.55, 2.69, and 3.52 μM, respectively; however, they also exhibited greater cytotoxicities with CC_{50} values of 69.5, 26.5, and 70.8 μM. Compound **27**, which has a methoxy instead of a phenolic hydroxy group, exhibited significant activity and low cytotoxicity, with EC_{50}, CC_{50}, and SI values of 1.72 μM, >200 μM, and 116.4, respectively. Similarly, when the phenolic hydroxy group of compound **3** was *O*-methylated as in compound **26**, the activity increased by 2-fold and the cytotoxicity decreased by 3-fold. The same trend was also observed in the sesquineolignan series. Compounds **23** and **24**, which do not possess a phenolic hydroxy moiety, exhibited significant inhibition with EC_{50} (SI) values of 1.70 (65.0) and 1.09 (41.1) μM, respectively. Compound **19**, which has two phenolic hydroxy substituents, had an EC_{50} (SI) value of 6.95 μM (3.3). These data strongly suggested that the phenolic hydroxy group in the structures of the sesquineolignans and dineolignans increases cytotoxicity and decreases antiviral activity.

EXPERIMENTAL SECTION

General Experimental Procedures. Optical rotations were measured on a Perkin-Elmer 341 polarimeter. UV spectra were recorded using a Shimadzu UV2457 spectrophotometer. ECD spectra were obtained on an Applied Photophysics Chirascan spectrometer. IR spectra were recorded on a Bruker Tensor 37 infrared spectrophotometer. The ^{1}H (400 MHz), ^{13}C (100 MHz), and 2D NMR spectra were obtained on a Bruker AVANCE-400 using TMS as an internal reference. HRESIMS were acquired on a Shimadzu LCMS-IT-TOF, and the ESIMS data were measured on an Agilent 1200 series LC-MS/MS system. TLC analysis was carried out on silica gel plates (Marine Chemical Ltd., Qingdao, China). RP-C_{18} silica gel (Fuji, 40−75 μm), MCI gel (CHP20P, 75−150 μm, Mitsubishi Chemical Corporation, Tokyo, Japan), silica gel (200−300 Mesh Marine Chemical Ltd., Qingdao, China), and Sephadex LH-20 (GE Healthcare Bio-Sciences AB, Sweden) were used for column chromatography (CC). Analytical and semipreparative HPLC separation were carried out on an LC-20AT Shimadzu liquid chromatography system with a ZORBA SB-C_{18} column (250 × 9.4 mm, 5 μm) or an Agilent SB-C_{18} column connected with an SPD-M20A diode array detector.

Plant Material. The roots of *S. chinensis* were collected in the Yulin District, Guangxi Province, China, and authenticated by Chunyan Han (Kunming Institute of Botany, CAS, China). A voucher specimen (No. 20120301) was deposited in the School of Pharmaceutical Sciences, Sun Yat-sen University, Guangzhou, China.

Extraction and Isolation. The air-dried and milled roots of *S. chinensis* (5 kg) were extracted by maceration in 95% EtOH (3 × 10 L) at room temperature for two days. The solvent was evaporated under reduced pressure to yield a crude extract (296 g), which was suspended in H_2O and extracted with petroleum ether (3 × 3 L), EtOAc (3 × 3 L), and *n*-BuOH (3 × 3 L). The EtOAc-soluble extract exhibited significant activity against EBV lytic replication, with an EC_{50} value of 21.31 μg/mL in HR-1 cell lines. Bioactivity-guided fractionation of the EtOAc-soluble (Fr. EA) extract was carried out using an anti-EBV assay in the P3HR-1 cell line. Fr. EA (96 g) was chromatographed on a silica gel column (800 g, 100−200 mesh, 10 × 70 cm) eluting with a step gradient of petroleum ether−EtOAc to give nine fractions (F1−F9). F2, F3, and F4 were the most active, and F2 (6.8 g) was further separated on another silica gel column using petroleum ether−EtOAc (90:10) as the mobile phase to yield five subfractions (F201 to F205). Compounds **17** (120.0 mg) and **22** (230.0 mg) were obtained from F203 by column chromatography on silica gel eluting with petroleum ether−EtOAc (90:10). F204 was chromatographed over an open C_{18} column (2.6 × 40 cm) eluting with a MeOH−H_2O mixture (80:20) to yield four subfractions (F2041−F2044). F2041 and F2044 were purified using HPLC on a semipreparative RP-18 column, using MeOH−H_2O (55:45) as the solvent system, to afford **8** (5.0 mg), **10** (130.0 mg), **13** (8.0 mg), **15** (5.0 mg), **18** (35.0 mg), **19** (8.0 mg), and **23** (40.0 mg). F3 was chromatographed on Sephadex LH-20 eluting with $CHCl_3$−MeOH (50:50) to give four subfractions (F301−F304). F301 was purified by RP-HPLC using MeOH−H_2O (55:45) as the solvent system to obtain **2** (9.0 mg), **9** (5.0 mg), **11** (15.0 mg), and **25** (14.0 mg). F302 was subjected to silica gel column chromatography eluting with CH_2Cl_2−MeOH (100:1) to obtain **26** (600.0 mg) and **27** (600.0 mg). F303 was purified by HPLC on a semipreparative RP-18 column using MeOH−H_2O (55:45) as the solvent to afford **3** (10.0 mg), **4** (40.0 mg), **14** (15.0 mg), and **28** (30.0 mg). F304 was subjected to CC on Sephadex LH-20, eluting with MeOH, to afford compounds **1** (12.0 mg) and **24** (800.0 mg). F4 was purified using MPLC, eluting with $CHCl_3$−MeOH (100:1), to give three subfractions (F401−F403). F402 was chromatographed over MCI gel eluting with an increasing gradient of MeOH (30−100%) in H_2O to give six subfractions (F4021−F4026). F4021 was subjected to a silica gel column eluting with a gradient of CH_2Cl_2−EtOAc to yield **5** (80.0 mg), **6** (13.0 mg), and **7** (15.0 mg). F4022 was purified by RP-HPLC using a mobile phase of MeOH−H_2O (55:45) to afford **12** (8.0 mg), **16** (6.0 mg), **20** (15.0 mg), and **21** (10.0 mg).

*Saurucinol A (**1**):* white powder; $[\alpha]^{20}_D$ −288 (*c* 0.01, $CHCl_3$); UV (MeOH) λ_{max} (log ε) 212 (4.37), 230 (4.44), 280 (4.35) nm; ECD (MeOH) λ_{max} ($\Delta\varepsilon$) 217 (−0.07), 348 (−0.20), 375 (+0.01) nm; IR ν_{max}

dx.doi.org/10.1021/np400757k | J. Nat. Prod. 2014, 77, 100−110

3449, 3367, 2924, 2853, 1658, 1511, 1261, 1219, 771 cm^{-1}; ^1H NMR ($CDCl_3$, 400 MHz) and ^{13}C NMR ($CDCl_3$, 100 MHz) data, see Table 1; HRESIMS *m/z* 753.2892 $[M+Na]^+$ (calcd for $C_{41}H_{46}O_{12}Na$, 753.2882).

*Saurucinol B (**2**):* white, amorphous solid; $[\alpha]^{20}_D$ −80 (*c* 0.01, $CHCl_3$); UV (MeOH) λ_{max} (log ε) 214 (4.28), 233 (4.37), 279 (4.00) nm; ECD (MeOH) λ_{max} ($\Delta\varepsilon$) 207 (−0.10), 283 (−0.10) nm; IR (KBr) ν_{max} 3477, 2925, 2853, 1660, 1512, 1264, 1219, 1035, 771 cm^{-1}; ^1H NMR ($CDCl_3$, 400 MHz) and ^{13}C NMR ($CDCl_3$, 100 MHz) data, see Table 1; positive mode HRESIMS *m/z* 747.3362 $[M + H]^+$ (calcd for $C_{42}H_{51}O_{12}$, 747.3375).

*4″-O-Demethylmanassantin A (**3**):* white, amorphous solid; $[\alpha]^{20}_D$ −35 (*c* 0.03, $CHCl_3$); UV (MeOH) λ_{max} (log ε) 210 (4.49), 231 (4.37), 280 (3.88) nm; ECD (MeOH) λ_{max} ($\Delta\varepsilon$) 220 (−0.17), 278 (−0.05) nm; IR (KBr) ν_{max} 3483, 2963, 2930, 1512, 1263, 1219, 1031, 771 cm^{-1}; ^1H NMR ($CDCl_3$, 400 MHz) and ^{13}C NMR ($CDCl_3$, 100 MHz) data, see Table 1; HRESIMS *m/z* 741.3245 $[M + Na]^+$ (calcd for $C_{41}H_{50}O_{11}Na$, 741.3294).

*3″-O-Demethylmanassantin B (**4**):* white, amorphous solid; $[\alpha]^{20}_D$ −112 (*c* 0.02, $CHCl_3$); UV (MeOH) λ_{max} (log ε) 208 (4.44), 231 (4.03), 286 (3.61) nm; ECD (MeOH) λ_{max} ($\Delta\varepsilon$) 220 (−0.07), 290 (−0.03) nm; IR (KBr) ν_{max} 3499, 2963, 2926, 1596, 1506, 1452, 1262, 1035, 755 cm^{-1}; ^1H NMR ($CDCl_3$, 400 MHz) and ^{13}C NMR ($CDCl_3$, 100 MHz) data, see Table 1; HRESIMS *m/z* 725.2950 $[M + Na]^+$ (calcd for $C_{40}H_{46}O_{11}Na$, 725.2932).

*Saurucinol C (**5**):* white powder; $[\alpha]^{20}_D$ +44 (*c* 0.01, $CHCl_3$); UV (MeOH) λ_{max} (log ε) 228 (4.36), 271 (4.34) nm; ECD (MeOH) λ_{max} ($\Delta\varepsilon$) 217 (−0.07), 358 (+0.24) nm; IR (KBr) ν_{max} 3743, 3361, 3193, 2923, 2853, 1658, 1583, 1462, 1416, 1330, 1236, 1126 cm^{-1}; ^1H NMR ($CDCl_3$, 400 MHz) and ^{13}C NMR ($CDCl_3$, 100 MHz) data, see Table 2; HRESIMS *m/z* 455.1651 $[M + Na]^+$ (calcd for $C_{23}H_{28}O_8Na$, 455.1676).

*Saurucinol D (**6**):* white powder; $[\alpha]^{20}_D$ −40 (*c* 0.02, $CHCl_3$); UV (MeOH) λ_{max} (log ε) 228 (4.10), 270 (3.33) nm; ECD λ_{max} ($\Delta\varepsilon$) (MeOH) 209 (−0.06), 282 (−0.05) nm; IR (KBr) ν_{max} 3744, 2923, 2852, 1741, 1512, 1462, 1366, 1220, 771 cm^{-1}; ^1H NMR ($CDCl_3$, 400 MHz) and ^{13}C NMR ($CDCl_3$, 100 MHz) data, see Table 2; HRESIMS *m/z* 499.1904 $[M + Na]^+$ (calcd for $C_{25}H_{32}O_9Na$, 499.1939).

*Saurucinol E (**7**):* white powder; $[\alpha]^{20}_D$ −34 (*c* 0.02, $CHCl_3$); UV (MeOH) λ_{max} (log ε) 228 (4.15), 268 (4.15) nm; ECD λ_{max} ($\Delta\varepsilon$) (MeOH) 212 (−0.04), 298 (−0.03) nm; IR (KBr) ν_{max} 3744, 3360, 2923, 2854, 1734, 1652, 1585, 1506, 1460, 1228, 1123, 771 cm^{-1}; ^1H NMR ($CDCl_3$, 400 MHz) and ^{13}C NMR ($CDCl_3$, 100 MHz) data, see Table 2; HRESIMS *m/z* 499.1969 $[M + Na]^+$ (calcd for $C_{25}H_{32}O_9Na$, 499.1939).

*Saurucinol F (**8**):* colorless oil; $[\alpha]^{20}_D$ −102 (*c* 0.01, $CHCl_3$); UV (MeOH) λ_{max} (logε) 225 (4.30), 266 (4.12) nm; ECD (MeOH) λ_{max} ($\Delta\varepsilon$) 216 (−0.03), 288 (−0.03), 348 (+0.01) nm; IR (KBr) ν_{max} 3465, 3362, 2922, 2851, 1633, 1219, 1126, 772 cm^{-1}; ^1H NMR ($CDCl_3$, 400 MHz) and ^{13}C NMR ($CDCl_3$, 100 MHz) data, see Table 2; HRESIMS *m/z* 425.1571 $[M + Na]^+$ (calcd for $C_{22}H_{26}O_7Na$, 425.1571).

*Saurucinol G (**9**):* colorless oil; $[\alpha]^{20}_D$ −111 (*c* 0.02, $CHCl_3$); UV (MeOH) λ_{max} (log ε) 214 (4.54), 271 (2.97) nm; ECD (MeOH) λ_{max} ($\Delta\varepsilon$) 283 (−0.01) nm; IR (KBr) ν_{max} 3449, 2932, 1632, 1590, 1501, 1425, 1225, 1124, 1039, 770 cm^{-1}; ^1H NMR ($CDCl_3$, 400 MHz) and ^{13}C NMR ($CDCl_3$, 100 MHz) data, see Table 2; HRESIMS *m/z* 425.1585 $[M + Na]^+$ (calcd for $C_{22}H_{26}O_7Na$, 425.1571).

*(−)-(7R,8R)-7-O-Acetylraphidecursinol B (**10**):* white, amorphous solid; $[\alpha]^{20}_D$ −18 (*c* 0.04, $CHCl_3$); UV (MeOH) λ_{max} (log ε) 217 (4.37), 270 (3.40) nm; ECD (MeOH) λ_{max} ($\Delta\varepsilon$) 230 (+0.04) nm; IR (KBr) ν_{max} 2961, 2839, 1589, 1502, 1459, 1422, 1234, 1125, 1026 cm^{-1}; ^1H NMR ($CDCl_3$, 400 MHz) and ^{13}C NMR ($CDCl_3$, 100 MHz) data, see Table 3; HRESIMS *m/z* 483.1988 $[M + Na]^+$ (calcd for $C_{25}H_{32}O_8Na$, 483.1989).

*(−)-(7R,8R)-7-O-Acetylpolysphorin (**11**):* white powder; $[\alpha]^{20}_D$ −24 (*c* 0.02, $CHCl_3$); UV (MeOH) λ_{max} (log ε) 222 (4.15), 268 (4.15) nm; ECD (MeOH) λ_{max} ($\Delta\varepsilon$) 239 (+0.01), 296 (−0.01) nm; IR (KBr) ν_{max} 2934, 2841, 1739, 1586, 1502, 1461, 1419, 1372, 1334, 1237, 1126, 761 cm^{-1}; ^1H NMR ($CDCl_3$, 400 MHz) and ^{13}C NMR ($CDCl_3$, 100 MHz) data, see Table 3; HRESIMS *m/z* 483.2019 $[M + Na]^+$ (calcd for $C_{25}H_{32}O_8Na$, 483.1989).

*(+)-(8R)-(2,6-Dimethoxy-4-propenylphenoxy)-1-(3,4,5-trimethoxyphenyl)propan-1-one (**12**):* white powder; $[\alpha]^{20}_D$ +48 (*c* 0.03, $CHCl_3$); UV (MeOH) λ_{max} (log ε) 222 (4.11), 281 (4.01) nm; ECD (MeOH) λ_{max} ($\Delta\varepsilon$) 365 (+0.12) nm; IR (KBr) ν_{max} 2932, 2839, 1680, 1645, 1500, 1459, 1330, 1233, 1126 cm^{-1}; ^1H NMR ($CDCl_3$, 400 MHz) and ^{13}C NMR ($CDCl_3$, 100 MHz) data, see Table 3; HRESIMS *m/z* 439.1737 $[M + Na]^+$ (calcd for $C_{23}H_{28}O_7Na$, 439.1727).

*(−)-(7R,8R)-Machilin D (**13**):* colorless oil; $[\alpha]^{20}_D$ −88 (*c* 0.02, $CHCl_3$); UV (MeOH) λ_{max} (log ε) 211 (4.41), 267 (4.07) nm; ECD (MeOH) λ_{max} ($\Delta\varepsilon$) 220 (−0.02) nm; IR (KBr) ν_{max} 3499, 2929, 1510, 1458, 1264, 1223, 1130, 1034, 769 cm^{-1}; ^1H NMR ($CDCl_3$, 400 MHz) and ^{13}C NMR ($CDCl_3$, 100 MHz) data, see Table 3; HRESIMS *m/z* 367.1532 $[M + Na]^+$ (calcd for $C_{20}H_{24}O_5Na$, 367.1516).

*Saurucinol H (**14**):* colorless oil; $[\alpha]^{20}_D$ −13 (*c* 0.02, $CHCl_3$); UV (MeOH) λ_{max} (log ε) 237 (4.05), 277 (3.68) nm; ECD (MeOH) λ_{max} ($\Delta\varepsilon$) 217 (−0.03), 289 (−0.03) nm; IR (KBr) ν_{max} 3361, 2925, 2852, 1608, 1513, 1460, 1216, 1115, 1028, 759 cm^{-1}; ^1H NMR ($CDCl_3$, 400 MHz) and ^{13}C NMR ($CDCl_3$, 100 MHz) data, see Table 4; HRESIMS *m/z* 411.1778 $[M + Na]^+$ (calcd for $C_{22}H_{28}O_6Na$, 411.1755).

*4-O-Methylsaurucinol H (**15**):* white, amorphous solid; $[\alpha]^{20}_D$ −8.9 (*c* 0.05, $CHCl_3$); UV (MeOH) λ_{max} (log ε) 215(4.32), 227 (4.27), 277 (3.68) nm; ECD (MeOH) λ_{max} ($\Delta\varepsilon$) 226 (−0.15), 277 (−0.09) nm; IR (KBr) ν_{max} 2925, 2850, 1591, 1509, 1459, 1262, 1229, 1127, 1019, 769 cm^{-1}; ^1H NMR ($CDCl_3$, 400 MHz) and ^{13}C NMR ($CDCl_3$, 100 MHz) data, see Table 4; HRESIMS *m/z* 425.1954 $[M + Na]^+$ (calcd for $C_{23}H_{30}O_6Na$, 425.1935).

*Saurucinol I (**16**):* colorless oil; $[\alpha]^{20}_D$ −1.8 (*c* 0.06, $CHCl_3$); UV (MeOH) λ_{max} (log ε) 217 (4.42), 273 (3.31) nm; ECD (MeOH) λ_{max} ($\Delta\varepsilon$) 226 (−0.05), 277 (−0.03) nm; IR (KBr) ν_{max} 2961, 2840, 1633, 1591, 1507, 1456, 1220, 1128, 772 cm^{-1}; ^1H NMR ($CDCl_3$, 400 MHz) and ^{13}C NMR ($CDCl_3$, 100 MHz) data, see Table 4; HRESIMS *m/z* 439.1740 $[M + Na]^+$ (calcd for $C_{23}H_{28}O_7Na$, 439.1727).

*Saurucinol J (**17**):* white, amorphous solid; $[\alpha]^{20}_D$ −10 (*c* 0.05, $CHCl_3$); UV (MeOH) λ_{max} (log ε) 220 (4.09), 271 (3.29) nm; ECD (MeOH) λ_{max} ($\Delta\varepsilon$) 223 (−0.03), 277 (−0.02) nm; IR (KBr) ν_{max} 3449, 2960, 2937, 2840, 1591, 1514, 1462, 1219, 1121, 1011, 772 cm^{-1}; ^1H NMR ($CDCl_3$, 400 MHz) and ^{13}C NMR ($CDCl_3$, 100 MHz) data, see Table 4; HRESIMS *m/z* 441.1909 $[M + Na]^+$ (calcd for $C_{23}H_{30}O_7Na$, 441.1884).

*Saurucinol K (**18**):* white, amorphous solid; $[\alpha]^{20}_D$ +63 (*c* 0.01, $CHCl_3$); UV (MeOH) λ_{max} (logε) 210 (4.31), 230 (4.18), 277 (3.71) nm; ECD (MeOH) λ_{max} ($\Delta\varepsilon$) 223 (−0.16), 275 (−0.08) nm; IR (KBr) ν_{max} 3499, 2961, 2929, 1608, 1514, 1458, 1262, 1221, 1030, 772 cm^{-1}; ^1H NMR ($CDCl_3$, 400 MHz) and ^{13}C NMR ($CDCl_3$, 100 MHz) data, see Table 4; HRESIMS *m/z* 381.1686 $[M + Na]^+$ (calcd for $C_{21}H_{26}O_5Na$, 381.1672).

*(-)-(7″R,8″R)-Saucerneol J (**19**):* white powder; $[\alpha]^{20}_D$ −86 (*c* 0.02, $CHCl_3$); UV (MeOH) λ_{max} (log ε) 212 (4.27), 231 (4.28), 280 (3.89) nm; ECD (MeOH) λ_{max} ($\Delta\varepsilon$) 220 (−0.02), 278 (−0.01) nm; IR (KBr) ν_{max} 3499, 2961, 1607, 1513, 1459, 1376, 1269, 1224, 1132, 1032, 764 cm^{-1}; ^1H NMR ($CDCl_3$, 400 MHz) and ^{13}C NMR ($CDCl_3$, 100 MHz) data, see Table 1; HRESIMS *m/z* 547.2334 $[M + Na]^+$ (calcd for $C_{30}H_{36}O_8Na$, 547.2302).

Preparation of (*R*)- and (*S*)-MTPA Esters of 1, 9, 13, and 19. Compound (1 mg) was dissolved in 1 mL of pyridine and stirred at rt for 10 min. An excess of (*R*)- or (*S*)-MTPA chloride (10 μL) was added, and the reaction was stirred overnight at rt. The solvent was removed in vacuo, and the crude reaction product was purified by preparative silica gel TLC using petroleum ether−EtOAc (5:1) as developing solvent.

^1H NMR data of (*R*)-MTPA ester of **1** (400 MHz, $CDCl_3$): δ_H 7.61 (2H, s, H-6, H-6′), 7.49 (2H, s, H-2, H-2′), 6.90−6.70 (8H, m, Ar-H), 6.06 (1H, d, *J* = 8.6 Hz, H-7″), 5.99 (1H, d, *J* = 8.5 Hz, H-7‴), 5.96 (2H, s, OCH_2O), 4.73 (1H, m, H-8″), 4.72 (1H, m, H-8‴), 3.87 (3H, 4″-OCH_3), 3.70 (3H, 3″-OCH_3), 3.80 (6H, 3-OCH_3, 3′-OCH_3), 1.23 (6H, s, H-9, H-9′), 1.12 (6H, s, H-9″, H-9‴). ^1H NMR data of (*S*)-MTPA ester of **1** (400 MHz, $CDCl_3$): δ_H 7.57 (2H, t, *J* = 8.8 Hz, H-6, H-6′), 7.47 (2H, d, *J* = 4.3 Hz, H-2, H-2′), 6.97−6.77 (8H, m, Ar-H), 6.17 (1H, d, *J* = 7.2 Hz, H-7″), 6.12 (1H, d, *J* = 7.4 Hz, H-7‴), 5.97

dx.doi.org/10.1021/np400757k | *J. Nat. Prod.* 2014, 77, 100−110

(2H, d, J = 4.1 Hz, OCH_2O), 4.71 (1H, m, H-8″), 4.70 (1H, m, H-8‴), 3.87 (3H, 4″-OCH_3), 3.83 (3H, 3″-OCH_3), 3.79 (6H, 3-OCH_3, 3′-OCH_3), 1.28 (6H, d, J = 6.1 Hz, H-9, H-9′), 1.10 (6H, d, J = 5.8 Hz, H-9″, H-9‴).

^{1}H NMR data of (*R*)-MTPA ester of **9** (400 MHz, $CDCl_3$): δ_H 6.46 (2H, s, OCH_2O), 6.37 (2H, s, H-3′, H-5′), 6.04 (1H, d, J = 7.5 Hz, H-7), 5.94 (2H, s, H-2, H-6), 5.11 (1H, m, H-8′), 5.08 (1H, d, J = 8.5 Hz, H-9′), 4.51 (1H, m, H-8), 3.77 (3H, 3-OCH_3), 3.73 (6H, 2′-OCH_3, 6′-OCH_3), 3.32 (1H, d, J = 6.5 Hz, H-7′), 0.95 (1H, d, J = 6.4 Hz, H-9). ^{1}H NMR data of (*S*)-MTPA ester of **9** (400 MHz, $CDCl_3$): δ_H 6.68 (2H, d, J = 8.6 Hz, OCH_2O), 6.35 (2H, s, H-3′, H-5′), 6.21 (1H, d, J = 5.8 Hz, H-7), 5.94 (2H, s, H-2, H-6), 5.10 (1H, m, H-8′), 5.07 (1H, d, J = 8.2 Hz, H-9′), 4.43 (1H, m, H-8), 3.84 (3H, 3-OCH_3), 3.73 (6H, 2′-OCH_3, 6′-OCH_3), 3.30 (1H, d, J = 6.6 Hz, H-7′), 0.97 (1H, d, J = 6.1 Hz, H-9).

^{1}H NMR data of (*R*)-MTPA ester of **13** (400 MHz, $CDCl_3$): δ_H 6.98−6.82 (6H, m, Ar-H), 6.35 (1H, d, J = 14.9 Hz, H-7′), 6.15 (1H, m, H-8′), 6.11 (1H, d, J = 7.6 Hz, H-7), 4.62 (1H, m, H-8), 3.80 (3H, 3′-OCH_3), 3.67 (3H, 3-OCH_3), 1.88 (1H, d, J = 6.6 Hz, H-9′), 1.09 (1H, d, J = 6.2 Hz, H-9). ^{1}H NMR data of (*S*)-MTPA ester of **13** (400 MHz, $CDCl_3$): δ_H 7.06−6.77 (6H, m, Ar-H), 6.34 (1H, d, J = 15.9 Hz, H-7′), 6.24 (1H, d, J = 6.5 Hz, H-7), 6.14 (1H, m, H-8′), 4.60 (1H, m, H-8), 3.79 (3H, 3′-OCH_3), 3.72 (3H, 3-OCH_3), 1.87 (1H, d, J = 6.5 Hz, H-9′), 1.07 (1H, d, J = 6.4 Hz, H-9).

^{1}H NMR data of (*R*)-MTPA ester of **19** (400 MHz, $CDCl_3$): δ_H 7.38−6.79 (9H, m, Ar-H), 6.11 (1H, d, J = 7.4 Hz, H-7″), 5.13 (1H, d, J = 8.2 Hz, H-7), 4.61 (1H, m, H-8″), 4.46 (1H, d, J = 9.3 Hz, H-7′), 3.82 (3H, 3″-OCH_3), 3.74 (3H, 3′-OCH_3), 3.71 (3H, 3-OCH_3), 2.32 (1H, m, H-8), 1.75 (1H, m, H-8′), 1.10 (1H, m, H-9′), 1.08 (1H, m, H-9″), 0.65 (1H, d, J = 7.0 Hz, H-9). ^{1}H NMR data of (*S*)-MTPA ester of **19** (400 MHz, $CDCl_3$): δ_H 7.29−6.79 (9H, m, Ar-H), 6.23 (1H, d, J = 6.3 Hz, H-7″), 5.12 (1H, d, J = 8.4 Hz, H-7), 4.59 (1H, m, H-8″), 4.45 (1H, d, J = 8.9 Hz, H-7′), 3.82 (3H, 3″-OCH_3), 3.72 (3H, 3′-OCH_3), 3.70 (3H, 3-OCH_3), 2.23 (1H, m, H-8), 1.74 (1H, m, H-8′), 1.08 (1H, d, J = 6.5 Hz, H-9′), 1.07 (1H, d, J = 6.2 Hz, H-9″), 0.65 (1H, d, J = 6.9 Hz, H-9).

Computational Methods. The calculated ECD spectra were obtained by density functional theory (DFT) and time-dependent DFT (TD-DFT) using Gaussian 09 and analyzed using GUIs GaussView (version 5.0). The calculated ECD spectra calculations were first performed at the HF/6-31G level in the gas phase for initial optimization. The minimum geometries were fully optimized at the B3LYP/6-31G(d) level in the gas phase to yield more accurate conformers. The ECD spectra were simulated at the B3LYP/6-31G(d,p) level in MeOH. The calculated ECD curve was generated using SpecDis with σ = 0.2 eV.

Analysis of Intracellular EBV Genomic DNA Content and Inhibition of EBV DNA Replication by Extracts and Compounds. P3HR-1 cells, a Burkitt lymphoma cell line latently infected with EBV, were cultured in RPMI 1640 medium (Gibco-BRL, Gaithersburg, MD, USA) supplemented with 10% fetal bovine serum (Gibco-BRL), streptomycin (100 μg/mL), and penicillin (100 units/mL). For viral lytic replication, P3HR-1 cells were induced with TPA (20 ng/mL) and sodium butyrate (0.3 mM). After three hours, the cells were treated with the extracts or compounds over a wide range of concentrations. Forty-eight hours postinduction, the total DNA in the cells was purified using the DNeasy tissue kit according to the manufacturer's protocol (Takara Bio. Inc., Japan). The EBV genomic copy number was quantified by real-time PCR on a Roche 480 LightCycler instrument using the LightCycler FastStart DNA Master^{plus} SYBR green kit with primers for the detection of EBNA1 (sense: 5′-CATTGAGTCGTCTCCCCTTTGGAAT-3′; antisense: 5′-TCATAACAAGGTCCTTAATCGCATC-3′). The half-maximal antiviral effective concentration (EC_{50}) value of each compound was determined from a dose−response curve of EBV DNA content values from TPA/butyrate-induced and compound-treated cells. The viral DNA contents were reduced by the contents of noninduced cells, divided by that from the control cells without drug treatment and then represented on the Y axes of the dose−response curves. Y axis value = (TPA_x − no TPA_x)/(TPA_0 − no TPA_0), where x is any concentration of the drug, and 0 represents no-drug treatment. The EC_{50} for viral DNA synthesis for each compound was calculated with the aid of GraphPad Prism software.

Cytotoxicity Assays. The viabilities of P3HR-1 cells after being treated or untreated with compounds were assessed by counting Trypan blue-stained cells two days post-treatment using a light microscope. Cell viabilities were defined relative to the control cells (nondrug treated). The half-maximal cytotoxic concentration (CC_{50}) was calculated from the dose−response curves with GraphPad Prism software.

■ ASSOCIATED CONTENT

Ⓢ Supporting Information

The IR, MS, 1D and 2D NMR, and CD spectra for compounds **1**−**19**. This material is available free of charge via the Internet at http://pubs.acs.org.

■ AUTHOR INFORMATION

Corresponding Authors

*E-mail: (Y. Yuan) yuan2@pobox.upenn.edu.

*E-mail: (Q. Gu) guqiong@mail.sysu.edu.cn. Tel: 86-20-39943077. Fax: 86-20-39943077.

Author Contributions

Hui Cui and Bo Xu contributed equally.

Notes

The authors declare no competing financial interest.

■ ACKNOWLEDGMENTS

This study was supported in part by the National High-Tech R&D Program of China (863 Program) (No. 2012AA020307), the R&D team program of Guangdong Province (No. 2009010058), the National Natural Science Foundation of China (No. 81001372, 81173470, 81271805, 81171575), the National Science and Technology Major Project of China (No. 2010ZX09102-305), and the External Cooperation Program of the Chinese Academy of Sciences (No. P2010-KF08).

■ REFERENCES

(1) Hwang, B. Y.; Lee, J. H.; Nam, J. B.; Hong, Y. S.; Lee, J. J. *Phytochemistry* **2003**, *64*, 765−771.

(2) Liu, J. B.; Wang, L. S.; Zhao, D. Q.; Cheng, D. Y.; Xu, T. H.; Zhou, X. F.; Yang, X. W.; Liu, Y. H. *Chem. Nat. Compd.* **2010**, *46*, 631−633.

(3) Lim, C. J.; Cuong, T. D.; Hung, T. M.; Ryoo, S.; Lee, J. H.; Kim, E. H.; Woo, M. H.; Choi, J. S.; Min, B. S. *Bull. Korean Chem. Soc.* **2012**, *33*, 3079−3082.

(4) Hodges, T. W.; Hossain, C. F.; Kim, Y. P.; Zhou, Y. D.; Nagle, D. G. *J. Nat. Prod.* **2004**, *67*, 767−771.

(5) Oh, K. S.; Choi, Y. H.; Ryu, S. Y.; Oh, B. K.; Seo, H. W.; Yon, G. H.; Kim, Y. S.; Lee, B. H. *Planta Med.* **2008**, *74*, 233−238.

(6) Chin, Y. W.; Cai, X. F.; Ahn, K. S.; Lee, H. K.; Oh, S. R. *Bull. Korean Chem. Soc.* **2010**, *31*, 2088−2090.

(7) Henle, G.; Henle, W. *J. Infect. Dis.* **1970**, *121*, 303−310.

(8) Heilmann, A. M.; Calderwood, M. A.; Johannsen, E. *J. Virol.* **2010**, *84*, 9920−9931.

(9) Chang, Y.; Chang, S. S.; Lee, H. H.; Doong, S. L.; Takada, K.; Tsai, C. H. *J. Gen. Virol.* **2004**, *85*, 1371−1379.

(10) Trumper, P. A.; Epstein, M. A.; Giovanella, B. C.; Finerty, S. *Int. J. Cancer* **1977**, *20*, 655−662.

(11) Raab-Traub, N.; Flynn, K. *Cell* **1986**, *47*, 883−889.

(12) Henle, G.; Henle, W. *Int. J. Cancer* **1976**, *17*, 1−7.

(13) Resnick, L.; Herbst, J. S.; Ablashi, D. V.; Atherton, S.; Frank, B.; Rosen, L.; Horwitz, S. N. *JAMA, J. Am. Med. Assoc.* **1988**, *259*, 384−388.

(14) Ernberg, I.; Bjorkholm, M.; Zech, L.; Sandstedt, B.; Szigeti, R.; Andersson, J.; Henle, W.; Klein, G. *J. Clin. Oncol.* **1986**, *4*, 1481−1488.

(15) Murakami, A.; Toyota, K.; Ohura, S.; Koshimizu, K.; Ohigashi, H. *J. Agric. Food Chem.* **2000**, *48*, 1518−1523.

(16) Iwatsuki, K.; Akihisa, T.; Tokuda, H.; Ukiya, M.; Oshikubo, M.; Kimura, Y.; Asano, T.; Nomura, A.; Nishino, H. *J. Nat. Prod.* **2003**, *66*, 1582−1585.

(17) Jimenez, I. A.; Bazzocchi, I. L.; Nunez, M. J.; Mukainaka, T.; Tokuda, H.; Nishino, H.; Konoshima, T.; Ravelo, A. G. *J. Nat. Prod.* **2003**, *66*, 1047−1050.
(18) Konoshima, T.; Okamoto, E.; Kozuka, M.; Nishino, H.; Tokuda, H.; Tanabe, M. *J. Nat. Prod.* **1988**, *51*, 1266−1270.
(19) Gu, Q.; Chen, Y. Y.; Cui, H.; Huang, D. N.; Zhou, J. W.; Wu, T. Z.; Chen, Y. P.; Shi, L. N.; Xu, J. *RSC Adv.* **2013**, *3*, 10168−10172.
(20) Gu, Q.; Wang, R. R.; Zhang, X. M.; Wang, Y. H.; Zheng, Y. T.; Zhou, J.; Chen, J. J. *Planta Med.* **2007**, *73*, 279−282.
(21) Xue, Y. B.; Zhang, Y. L.; Yang, J. H.; Du, X.; Pu, J. X.; Zhao, W.; Li, X. N.; Xiao, W. L.; Sun, H. D. *Chem. Pharm. Bull.* **2010**, *58*, 1606−1611.
(22) Greger, H.; Pacher, T.; Vajrodaya, S.; Bacher, M.; Hofer, O. *J. Nat. Prod.* **2000**, *63*, 616−620.
(23) Sung, S. H.; Huh, M. S.; Kim, Y. C. *Chem. Pharm. Bull. (Tokyo)* **2001**, *49*, 1192−1194.
(24) Hwang, B. Y.; Lee, J. H.; Nam, J. B.; Hong, Y. S.; Lee, J. J. *Phytochemistry* **2003**, *64*, 765−771.
(25) Seo, C. S.; Lee, W. H.; Chung, H. W.; Chang, E. J.; Lee, S. H.; Jahng, Y.; Hwang, B. Y.; Son, J. K.; Han, S. B.; Kim, Y. *Phytother. Res.* **2009**, *23*, 1531−1536.
(26) Hoye, T. R.; Jeffrey, C. S.; Shao, F. *Nat. Protoc.* **2007**, *2*, 2451−2458.
(27) Hanessian, S.; Reddy, G. J.; Chahal, N. *Org. Lett.* **2006**, *8*, 5477−5480.
(28) Lee, A. L.; Ley, S. V. *Org. Biomol. Chem.* **2003**, *1*, 3957−3966.
(29) Hada, S.; Hattori, M.; Tezuka, Y.; Kikuchi, T.; Namba, T. *Phytochemistry* **1988**, *27*, 563−568.
(30) Xiong, L.; Zhu, C.; Li, Y.; Tian, Y.; Lin, S.; Yuan, S.; Hu, J.; Hou, Q.; Chen, N.; Yang, Y.; Shi, J. *J. Nat. Prod.* **2011**, *74*, 1188−1200.
(31) Kim, K. H.; Kim, H. K.; Choi, S. U.; Moon, E.; Kim, S. Y.; Lee, K. R. *J. Nat. Prod.* **2011**, *74*, 2187−2192.
(32) Bezerra, A. D.; Lins, A. C. D.; de Athayde, P. F.; da Silva, M. S.; Barbosa, J. M.; Camara, C. A.; Silva, T. M. S.; Luna, V. D.; dos Santos, C. F. *Quim. Nova* **2012**, *35*, 2226−2228.
(33) Lopes, N. P.; Blumenthal, E. E. D.; Cavalheiro, A. J.; Kato, M. J.; Yoshida, M. *Phytochemistry* **1996**, *43*, 1089−1092.
(34) Huang, Y. T.; Chang, H. S.; Wang, G. J.; Cheng, M. J.; Chen, C. H.; Yang, Y. J.; Chen, I. S. *J. Nat. Prod.* **2011**, *74*, 1875−1880.
(35) Martins, R. C. C.; Latorre, L. R.; Sartorelli, P.; Kato, M. J. *Phytochemistry* **2000**, *55*, 843−846.
(36) Martins, R. C. C.; Lago, J. H. G.; Albuquerque, S.; Kato, M. J. *Phytochemistry* **2003**, *64*, 667−670.
(37) Li, Y. R.; Cheng, W.; Zhu, C. G.; Yao, C. S.; Xiong, L.; Tian, Y.; Wang, S. J.; Lin, S.; Hu, J. F.; Yang, Y. C.; Guo, Y.; Yang, Y.; Li, Y.; Yuan, Y. H.; Chen, N. H.; Shi, J. G. *J. Nat. Prod.* **2011**, *74*, 1444−1452.